LINKÖPING UNIVERSITY

Analytical Design and Estimation of Conventional and Electrical Aircraft Environmental Control Systems

Hemanth Devadurgam , Soorya Rajagopal , Raghu Chaitanya Munjulury

Division of Fluid and Mechatronic Systems,
Department of Management and Engineering,
Linköping University, Linköping, Sweden - 58183

ABSTRACT

Environmental control system holds vital importance as it is responsible for passenger's ventilation and comfort. This paper presents an analytical design of environmental control systems and represents the estimated design in three-dimensional. Knowledge-based engineering application serves as the base for designing and methodology for the environmental control systems. Flexibility in the model enables the user to control the size and positioning of the system and also sub-systems associated with it. The number of passengers serves as the driving input and three-dimensional model gives the exact representation with respect to the volume occupied and dependencies on the number of passengers. It also provides a faster method to alter the system to user needs with respect to the number of air supply pipes, number of ducts and pipe length. Knowledge-based engineering gives the freedom to visualize various options in the conceptual design process.

Nomenclature

Abbreviation	Meaning
ACM	Air Cycle Machine
cmp	Compressor
CATIA	Computer Aided Three Dimensional Interactive Application
ECS	Environmental Control System
HPWS	High Pressure Water Separation System
LPWS	Low Pressure Water Separation System
MHX	Main Heat Exchanger
PHX	Primary Heat Exchanger
RAPID	Robust Aircraft Parametric Interactive Design
trb	Turbine

Symbol	Description	Units
A	Area	m^2
P	Perimeter	m
T	Temperature	degree C
k	Thermal Conductivity	$\frac{kg}{mK}$
K	Kelvin	K
D	Hydraulic Diameter	m
m	Mass flow rate	$\frac{kg}{s}$
p	Pressure	Pa
μ	Dynamics viscosity	$\frac{kg}{ms}$

1 Introduction

The Environmental Control System (ECS) is responsible for passengers comfort and one of the most important systems of an aircraft. Temperature and pressure of the air vary on the altitude and ECS works on regulating the air, takes-in the bleed air mixes it with the recirculating air so that the pressure and temperature of the air are safe for breathing. Also, the system provides de-misting, anti-icing functions for the aircraft [1].

Conventional ECS, operates on an open loop system, with air acting as the refrigerant. Bleed air is conditioned and fed into the aircraft for passenger survival. Further, this system is classified as a Low-Pressure Water Separation System (LPWS) and High-Pressure Water Separation System (HPWS). A commonly used system in aircraft, where the air is used as a refrigerant. Air is made to pass through heat exchangers, Turbines, Condenser and water extraction loop to give the conditioned air.

The difference between LPWS and HPWS is the water extraction loop, consisting of Reheater and Condenser. Although LPWS has fewer components and lesser weight, the absence of water extraction loop unit becomes the limiting factor. The absence of this loop can lead to icing near the Turbine unit. This icing is not a desirable effect and thus, HPWS becomes the better choice and is used commercially on a large

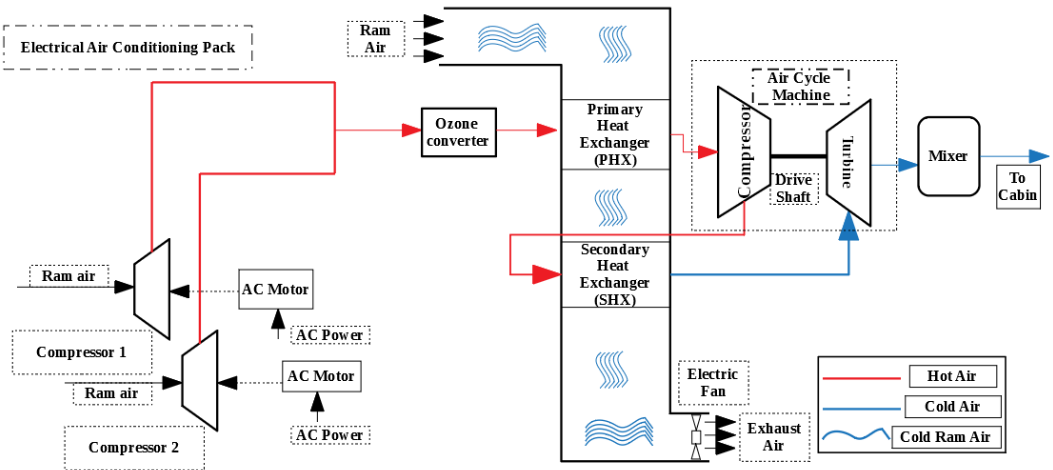

Fig. 1 . Electrical ECS Schematic diagram [1]

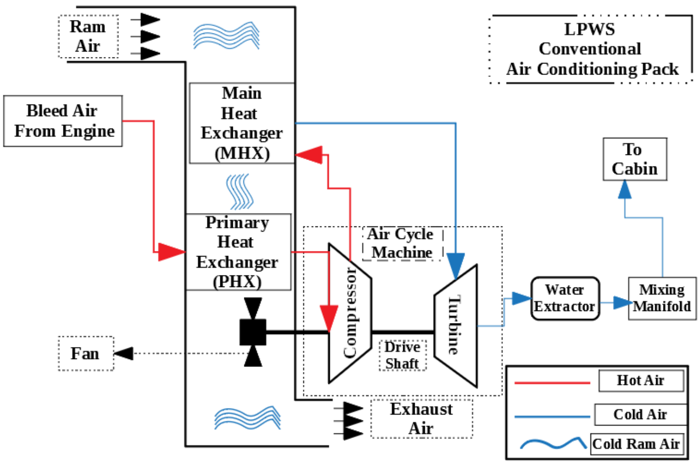

Fig. 2 . Low pressure water separation system schematic diagram [1]

scale.

On the other hand, electrical ECS mainly operates on reducing power consumption, by using electric power instead of pneumatic power. Air is taken as the ram-air substitute and is conditioned before feeding into the fuselage. Electrical ECS comprises of two air conditioning packs, which are electrically powered and motor driven. Electrical ECS is gaining importance due to the lesser fuel consumption and eco-friendliness when compared to the conventional ECS. Lack of bleed air inlet essentially means cabin pressurization is provided by electrical compressors. These compressors also act as the source of air for the ECS, illustrated in Figure 1.

2 Aims and Objectives

This paper aims at designing and sizing conventional & electrical ECS and air supply piping along with diffusers. These could be used for different sizes and types of aircraft with a varying number of passengers. The user gets the freedom to choose the type of ECS system along with the air supply piping and diffusers(single-aisle). While fulfilling the goals, the objectives considered were,

- Designing the ECS and components based on the type of aircraft or number of passengers.
- Calculate inlet and outlet temperatures and pressures of individual components.
- Validating the outputs temperatures (K) and pressures (Pa) of bleed air.
- Designing air supply piping for single and double aisle configurations, which could be instantiated along the length of the fuselage.

3 Methodology

The various components that make an ECS are sized/modeled and presented below. Also, the as-

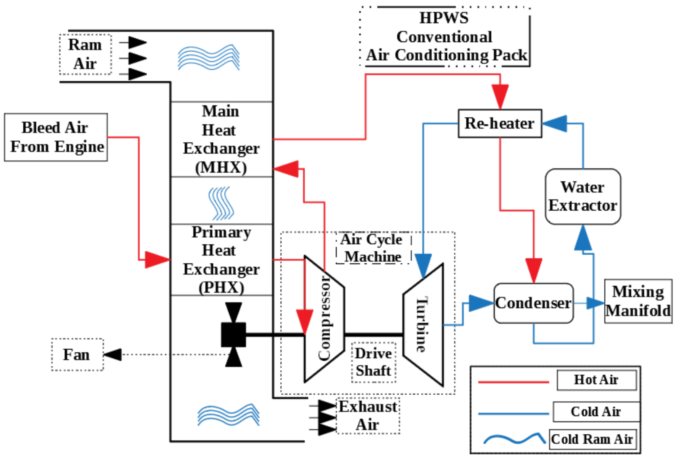

Fig. 3 . High pressure water separation system schematic diagram [1]

sisting equations are illustrated with numerical values along with the assumptions made to in the design process. Initial assumptions are based on Moir & Seabridge [1]:

- Cruising altitude of 11277m
- Mach number of 0.78
- Inlet bleed air temperature at PHX (T_{bleed}) is 473.15 K
- Ram air temperature (T_{ram}) is 217.15 K

3.1 Analytical component sizing

Heat exchangers form the backbone of ECS. Cross-flow heat exchangers are considered and only dry bleed air is made to pass through the ECS[2]. Each component of ECS is illustrated with the sizing equations along with the assumptions. These equations increase the flexibility and adaptability of the system. The number of passengers (N_{Pax}) acts as the driving input for the ECS sizing. Other limitations like stresses, size, servicing, material, and cost were neglected during the sizing/modeling of the individual ECS components.

3.1.1 Heat Exchanger

The Primary heat exchanger (PHX) & Main heat exchanger(MHX) are not the only heat exchangers in ECS, even Reheater & Condenser are also cross-flow type heat exchangers. Thus, PHX, MHX, Reheater, and Condenser have the same sizing equations. These are discussed in this section with emphasis on the method employed for the sizing.

- Fin tube hydraulic diameter on hot and cold side of the heat exchanger [2].

$$D_h = \frac{4A_t}{P_t} \quad (1)$$

where,

- A_t = Inside cross section area of the tube, (m^2)
- P_t = Perimeter of the tube, (m)

- Density of air on hot and cold side of the heat exchanger [2].

$$\rho = \frac{MP}{RT} \quad (2)$$

where,

- ρ = Density, ($\frac{Kg}{m^3}$)
- M = Molar mass of the air = 29
- P = Pressure of air, (bar)
- R = Gas constant=0.0831 ($\frac{J}{mol.K}$)
- T = Temperature of air, (K)

- For dynamic viscosity, Sutherland's law is used [2].

$$\mu = \mu_{ref} * (\frac{T}{T_{ref}})^{1.5} * (\frac{T_{ref}+S}{T+S}) \quad (3)$$

where,

- μ = Dynamic Viscosity, ($\frac{Kg}{m.s}$)

- μ_{ref} = Reference Dynamic Viscosity, $(\frac{Kg}{m.s})$
- T = Temperature of air, (K)
- T_{ref} = Temperature of air at sea level, (K)
- S = Sutherland's Temperature, (K)

Gas	μ_{ref} $(\frac{Kg}{m}).s$	T_{ref} (K)	S (K)
Air	$1.76*10^{-5}$	288.15	110.4

Table 3. Sutherland's Constant

- Flow velocity of air on hot and cold side of the heat exchanger [3].

$$V = \frac{m}{\rho * A} \quad (4)$$

where,

- V = Flow Velocity of air, $(\frac{m}{s})$
- ρ = Density, $(\frac{Kg}{m^3})$
- A = Cross sectional area of the tube = $(P_t * D_h)/4$, (m^2)
- m = Mass flow rate of air, $(\frac{Kg}{s})$

- Reynolds number of air on hot side and cold side of the heat exchanger [2].

$$Re = \frac{\rho * V * D_h}{\mu} \quad (5)$$

where,

- V = Flow Velocity of air, $(\frac{m}{s})$
- ρ = Density, $(\frac{Kg}{m^3})$
- D_h = Hydraulic Diameter of the tube, (m)
- μ = Dynamic Viscosity, $(\frac{Kg}{m.s})$

- Thermal conductivity of air on hot side and cold side of the heat exchanger (W/m.K) [2].

$k_{air} = (((1.52*10^{-11})*(T_{bleed}^3)) - ((4.86*10^{-8})*$

(T_bleed^2))+((1.02*10^-4)*(T_bleed))-(3.93*10^-4)) (6)

- Prandtl number of air on cold and hot side of the heat exchanger [4].

$$Pr = (\mu * C_p)/K_{air} \quad (7)$$

- Nusselt number of air [2].

$$f = (0.790*(log(Re)) - (1.64))^{-2} \quad (8)$$

$$Nu = ((f/8)*(Re-1000)*Pr)/(1+12.7*((f/8)^{0.5})*(Pr^{\frac{2}{3}})-1 \quad (9)$$

- Heat transfer coefficient $(\frac{W}{m^2}K)$ of hot and cold side of the heat exchanger [3].

$$h = (Nu * K_{air})/(D_h) \quad (10)$$

- Number of tube passes in the heat exchanger [3].

$$N_t = (L_a - D_h)/S_L \quad (11)$$

where,

- S_L = Longitudinal fin pitch distance, (m)

- Total heat transfer area at hot and cold side of the heat exchanger [2] .

$$A_{HS} = 2*(N_t)*(L_b)*(L_c)*(((s_f - Th_f)+(2*fin_h))/s_f) \quad (12)$$

$$A_{CS} = 2*(N_t)*(L_a)*(L_b)*(((s_f - Th_f)+(2*fin_h))/s_f) \quad (13)$$

where,

- N_t = Number of tube passes
- fin_h = Fin height in, (m)
- Th_f = fin thickness, (m)
- L_a, L_b, L_c are the length,breadth and height, (m)

- Total surface temperature effectiveness of fin [4].

$$E_{ft} = 1 - ((1 - \eta_{fin}))*(A_{HS}/A_{CS})) \quad (14)$$

where,

- η_{fin} = Isentropic efficiency of fin

- Overall thermal resistance [4].

$R_{TR} = (1/(E_{ft}*h)) + (1/((A_{hs}/volume_{hx})$

/(A_hs/volume_hx)*h))+((T_hf/ K_fin)) (15) where,

- K_{fin} = Thermal conductivity of fin , $(\frac{W}{mK})$
  - $volume_{hx}$ = $(L_a)*(L_b)*(L_c)$, (m^3)
- Overall heat transfer coefficient [4].

$$U = (1/R_{TR}) \quad (16)$$

- Heat capacity rate for both bleed and ram air [3].

$$Ca_{(max/min)} = m_{(bleed/Ram)} * C_p \quad (17)$$

where,

- m=Mass flow rate of bleed air or ram air, $(\frac{Kg}{sec})$
- C_p = Specific heat of air at constant pressure, $((\frac{J}{kg.K}))$
- Stream heat capacity rate ratio (dimensionless value between 0 and 1) [3].

$$Ca_R = (Ca_{max(bleed/ram)}/Ca_{min(bleed/ram)}) \quad (18)$$

- Number of transfer units, [3].

$$NTU = (U * A_{CS})/(Ca_{min(bleed/ram)}) \quad (19)$$

- Effectiveness of the heat exchanger [4].

$$E = (1 - exp((exp(-Ca_R*(NTU^{0.78})) - 1)/$$

(Ca_R*NTU^-0.22))) (20)

- Total heat transfer rate [4].

$$Q = (E)*(Ca_{min(bleed/ram)})*(T_{bleed} - T_{ram}) \quad (21)$$

$$Ca_{min} = min(Ca_{max(bleed/ram)}, Ca_{min(bleed/ram)}) \quad (22)$$

- Tube length per pass [3].

$$L_{tube} = (NTU*Ca_{max(bleed/ram)})/(U*N*2*\pi*D_h) \quad (23)$$

- Bleed air outlet temperature (K) from heat exchanger [4].

$$T_{phx} = (T_{bleed}) - (Q/Ca_{min(bleed/ram)}) \quad (24)$$

- Pressure drop at the heat exchanger [4].

$$U_m = (4*m)/((rho*\pi*(D_h^2))) \quad (25)$$

$$fric_{coeff} = (1.58*(log(Re)) - (3.28))^{-2} \quad (26)$$

$$\Delta P = (fric_{coeff}*((rho*(U_m^2))/(2*D_h)))*L_{tube} \quad (27)$$

- Outlet pressure from PHX (Inlet pressure to compressor) [3].

$$P_{out} = P_{in} - \Delta P \quad (28)$$

3.1.2 Compressor

It is essential to find the work done by the compressor and the radial speed of the impeller as part of the air cycle machine that takes in cold bleed air from the engine, pressurizes and increases the temperature of the bleed air.

The outlet temperature of the compressor,

$$T_{cmpout} = T_{cmpin}*(\pi_c)^{((g-1)/g)} \quad (29)$$

It is also important to find the is-entropic temperature of the compressor,

$$T_{cmpis} = (T_{cmpout} - T_{cmpin} + (\eta_{cmp}*T_{cmpin}))/\eta_{cmp} \quad (30)$$

Work done by the compressor,

$$W_{cmp} = m*(C_p)*(T_{cmpis} - T_{cmpin}) \quad (31)$$

Radial speed of the impeller,

$$U_2 = ((W_{cmp}*1000)/S_{fcmp}^{0.5} \quad (32)$$

Outlet pressure of the compressor,

$$P_{cmpout} = \pi_c * P_{cmpin} \quad (33)$$

For electric ECS, pressure of ram air at the inlet is obtained by considering the aerodynamic effects while the aircraft is cruising.

$$P_{cmpin(e-ecs)} = P_{atm}*(1+0.2*Ma^2)^{3.5} \quad (34)$$

3.1.3 Turbine

Turbine is another essential component of the air cycle machine. The temperature of the air drops as the air expands through the Turbine. Work done by the Turbine and the radial speed of the impeller is to be calculated for the model. The outlet temperature and pressure of the Turbine are given by Equations 36 and 39 respectively.

Outlet temperature of the Turbine,

$$T_{trbOut} = T_{trbIn} * (1 - (\eta_{trb} * (1 - (\pi_{trb})^{(}(g-1)/g)))) \quad (35)$$

Isentropic temperature,

$$T_{trbIs} = (T_{trbOut} - T_{trbIn} + (\eta_{trb} * T_{trbIn}))/\eta_{trb} \quad (36)$$

Work-done by the Turbine,

$$W_{trb} = (m) * (C_p) * (T_{trbIn} - T_{trbIs}) \quad (37)$$

Radial speed of the impeller,

$$U_{2trb} = ((W_{trb} * 1000)/Sf_{trb})^{0.5} \quad (38)$$

Outlet pressure of the Turbine,

$$P_{trbOut} = \pi_{trb} * P_{trbIn} \quad (39)$$

3.1.4 Pressure Losses in Pipes

In general, the pressure loss is considered for all types of fully developed flows i.e., laminar or turbulent, circular or non-circular, smooth or rough surfaces, horizontal or inclined pipes. There are different kinds of pressure losses and the equations that were used to compute them are presented in this section.

1. Pressure loss in the pipe

$$\Delta P_L = (\rho) * (g) * (h_L) \quad (40)$$

2. Pressure loss at the pipe bends

- Head loss at the bend.

$$h_{L_{bend}} = (K_L) * (\frac{V^2}{2 * g}) \quad (41)$$

4 Results

Numerical data obtained for the different components of the conventional ECS are analyzed and validated in this section. Also, results obtained for the three different aircraft types that were considered are being evaluated. The performance of ECS varies with the user input called the number of passengers. The results obtained along with the assumptions made for the different components of the system are provided below.

$$\mathbf{m_{bleed} = N_{pax} * m_{pax}} \quad (42)$$

Aircraft Type (–)	**Number of passengers** (N_{pax})	**Bleed air mass flow rate** $(\frac{kg}{sec})$	**Ram air mass flow rate** $(\frac{kg}{sec})$
1	150	0.50	0.8
2	250	0.83	1.1
3	350	1.17	1.4

Table 4. Bleed and ram air mass flow rate

4.1 Conventional Environmental Control System

4.1.1 Heat Exchangers - PHX and MHX

Aircraft Type (–)	**L**$_{ap}$ **(m)**	**L**$_{bp}$ **(m)**	**L**$_{cp}$ **(m)**
1	0.25	0.23	0.15
2	0.30	0.25	0.15
3	0.32	0.20	0.18

Table 5. PHX geometry for three aircraft types

Aircraft Type (–)	**L**$_{am}$ **(m)**	**L**$_{bm}$ **(m)**	**L**$_{cm}$ **(m)**
1	0.25	0.23	0.15
2	0.30	0.25	0.15
3	0.32	0.20	0.18

Table 6. MHX geometry for three aircraft types

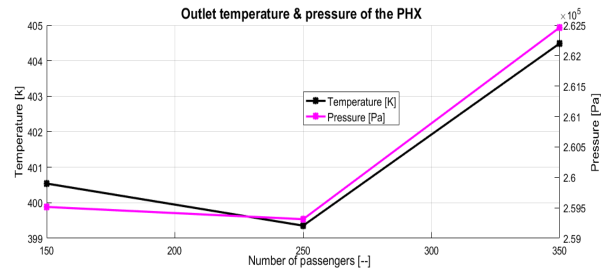

(a) PHX

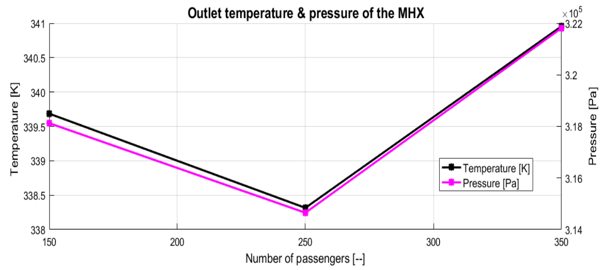

(b) MHX

Fig. 4 . Outlet Pressure and Temperature of the bleed air at the outlet of the PHX and MHX

The Primary heat exchanger (PHX) & Main heat exchanger(MHX) are typically cross-flow type heat exchangers. Depending on the inlet mass flow rate of the air the size of the component varies. As the aircraft type changes i.e., as the number of passengers increase the mass flow rate of hot bleed air increases and vice-versa.

For both PHX and MHX, the fin height and fin thickness are taken as 0.006 m and 0.0002 m respectively for all the three aircraft types [2]. The inside cross-sectional area (A_t) and perimeter of the tube (P_t) is taken as 0.002 m^2 and 0.54 m respectively [2]. The thermal conductivity of the fin (K_{fin}) is considered to be 177 ($\frac{W}{m^2}K$) [5] for all the aircraft.

4.1.2 Air Cycle Machine - Compressor & Turbine

The compressor, Turbine, and fan are all mounted on the same shaft and Turbine drive the compressor. Figure 5a and Table 7, represent the Turbine outlet temperature, pressure and the diameter of the compressor impeller for the aircraft types. The bleed air from the reheater cold side (CS) flows into the Turbine. Figure 5b and Table 8, represent the Turbine outlet temperature, pressure and the diameter of the impeller for the aircraft types.

Aircraft Type (–)	**Outlet Diameter D_2 (m)**	**Inlet Diameter D_1 (m)**
1	0.076	0.038
2	0.098	0.049
3	0.11	0.055

Table 7. The inlet and outlet geometry of the air cycle machine compressor impeller

Aircraft Type (–)	**Outlet Diameter D_2 (m)**	**Inlet Diameter D_1 (m)**
1	0.076	0.038
2	0.099	0.049
3	0.11	0.055

Table 8. The inlet and outlet geometry of the air cycle machine Turbine impeller

The values in Table 7, were obtained using sizing equation's considered in Section 3.1. The pressure ratio of the compressor (π_c) is considered to be 1.4 [2]. The specific heat of bleed air at constant pressure and volume is considered to be c_p=1.005 $(kj/kg.K)$ and c_v=0.716 $(kj/kg.K)$ [3]. The compressor efficiency (η_{cmp}) is assumed to be 0.7 [2]. Slip factor of the compressor (S_{fcmp}) is taken as 0.9 [6]. The impeller rotations per minute (rpm) (N_{cmp}) is considered to be 45000 [7]. The diffuser inlet diameter (D_{1cmp}) was assumed to be half of the (D_{2cmp}). The assumptions considered for the Turbine are as follows, the expansion ratio of the Turbine for all the three aircraft types is assumed to be 2. The slip factor of the Turbine is assumed to be 0.9. The isentropic efficiency of the Turbine is assumed to be 0.8 for all three aircraft types.

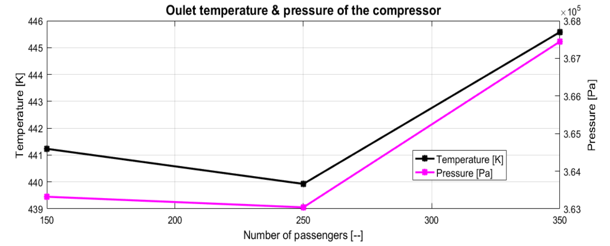

(a) Compressor

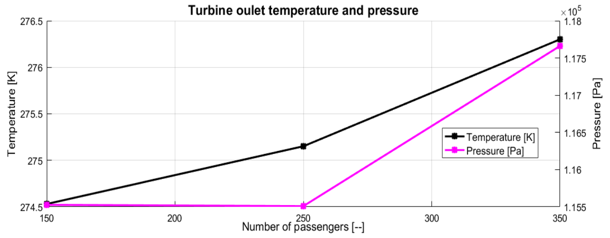

(b) Turbine

Fig. 5 . Outlet Pressure and Temperature of bleed air

4.1.3 High Pressure Water Separation Loop

The high-pressure water separation loop consists of Reheater, Condenser, Water extractor, and Turbine. The bleed air temperature and pressure at the cold side of the Reheater are assumed to be 320 K and 260000 Pa [2].

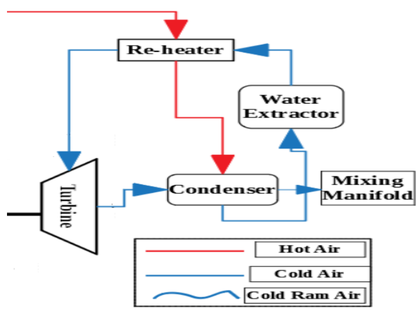

Fig. 6 . High pressure water separation loop Conventional ECS [1]

4.1.4 Reheater (Cold & Hot Side) & Condenser (Low pressure side (LPS) & High pressure Side (HPS))

Reheater (REH) and Condenser are cross-flow type heat exchangers. The bleed air from the MHX flows through the hot side of the Reheater. Bleed air from the high pressure side of the condenser flows into cold side of the Reheater. From Reheater hot side (HS), the bleed air flows into the high pressure side (HPS) of the condenser.

The Reheater geometry for three Aircraft types			
Aircraft Type (–)	**L_{aR} (m)**	**L_{bR} (m)**	**L_{cR} (m)**
1	0.10	0.10	0.10
2	0.14	0.14	0.14
3	0.18	0.18	0.18

Table 9. The above table illustrates the considered Reheater geometry for three aircraft types

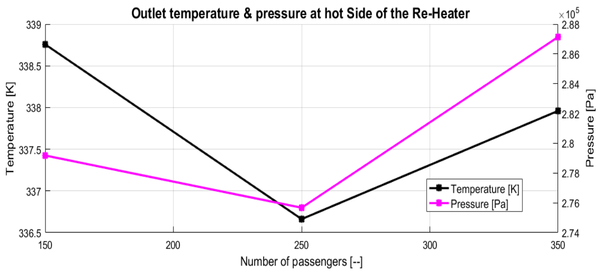

(a) Hot side

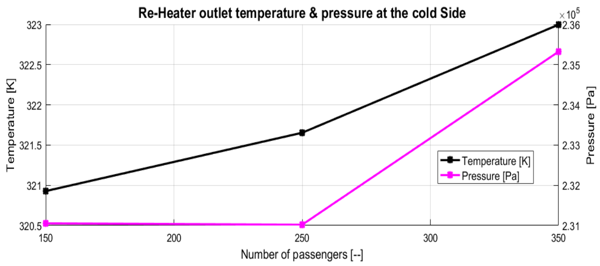

(b) Cold side

Fig. 7 . Outlet temperature & pressure of bleed air at outlet of the Reheater

Here, the Turbine outlet bleed air acts as the coolant air and passes to the low pressure side of the condenser. At high pressure side of the condenser, bleed air from Turbine outlet acts as the coolant and passes at the low pressure side of the condenser. The bleed air from the condenser high pressure side (HPS) flows into the Reheater cold side (CS).

The Condenser geometry for three Aircraft types			
Aircraft Type (–)	**L_{aC} (m)**	**L_{bC} (m)**	**L_{cC} (m)**
1	0.10	0.10	0.10
2	0.14	0.14	0.14
3	0.18	0.18	0.18

Table 10. The above table illustrates the considered Condenser geometry for three aircraft types

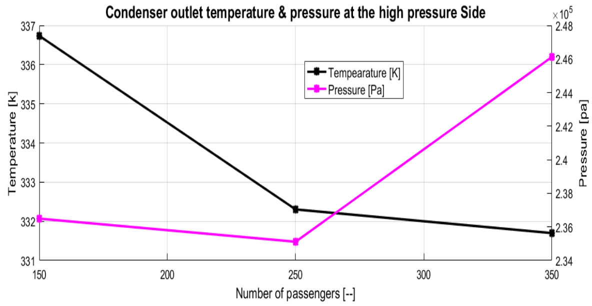

(a) High pressure side

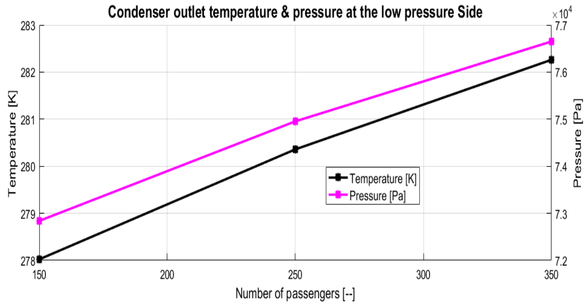

(b) Low pressure side

Fig. 8 . Outlet temperature & pressure of the Condenser

Bleed air from Turbine flows into the low pressure side of the condenser. Figure 8b & Figure 8a, represent the temperature and pressure of the bleed air at the exit of the condenser (low pressure side (LPS)) respectively. The heat transfer takes place between the bleed air flowing at the condenser high pressure side (HPS) and bleed air flowing at the low pressure side (LPS). Figure 7a & Figure 7b, represent the outlet temperature and pressure values of the bleed air at the exit of the hot and cold side of the Reheater respectively.

4.1.5 Validation of inlet and outlet temperature of ECS components

The summarizes of the inlet and outlet temperatures of different components of the conventional ECS are shown in Figure 9. The values are validated with Liebherr ECS data [8].

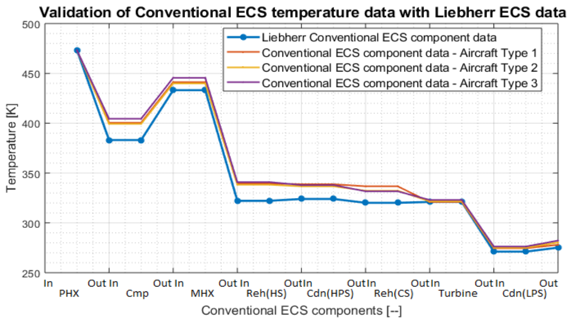

Fig. 9 . Validation of inlet and outlet Temperature of components vs Liebherr data [8]

4.2 Electrical ECS

The results for Electrical ECS, the sizing values with respect to individual components of the system are tabulated. Comparing with conventional ECS, components like Reheater, Condenser and Water extractor are absent. Components like compressors and fans are powered by motors running on AC power.

4.2.1 Ram Air Compressors

In Electric ECS, bleed air from the engine is absent. Instead ram air is used from atmosphere as the source of air to electric ECS, fed by electric ram air compressors.

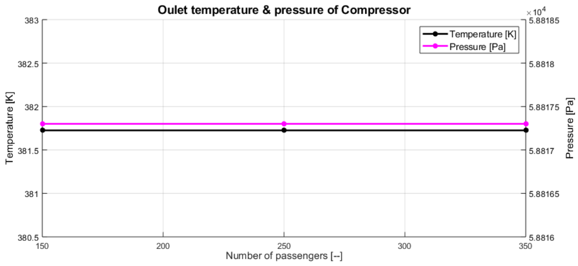

Fig. 10 . Temperature and pressure ram air outlet of two electric compressors

Aircraft Type (–)	Outlet Diameter D_2 (m)	Inlet Diameter D_1 (m)
1	0.14	0.07
2	0.18	0.09
3	0.21	0.105

Table 11. Inlet and Outlet geometry of the impeller

Compressed air passes through the ozone separator and flows into the Primary heat exchanger (PHX). The primary heat exchanger is a cross-flow type heat exchanger same as the conventional HPWS-ECS. The compressed hot ram air from ram air compressors passes at one side of PHX and cold ram air passes from the other side of the PHX from plenum.
The inlet pressure of the ram air is obtained using the inlet pressure Equation 34. The Mach number of the aircraft is considered to be 0.75 and is flying at an altitude of 11277.6 m. The atmospheric pressure(P_{atm}) at 11277.6 m is 8100 Pa [1]. Table 11 illustrates the impeller geometry of the compressor. Figure 10 illustrates the temperature and pressure of the ram air at the outlet of the compressor. The pressure ratio of the two ram air compressors is considered to be 5 [9]. The slip factor of the ram air compressors is considered to be 0.9 [6]. The isentropic efficiency of the ram air compressors is considered to be 0.7 [9].

4.2.2 Primary Heat Exchanger & Secondary Heat Exchanger

Aircraft Type (–)	L_{ap} (m)	L_{bp} (m)	L_{cp} (m)
1	0.13	0.11	0.11
2	0.22	0.20	0.20
3	0.27	0.25	0.25

Table 12. Electric ECS - PHX geometry for three aircraft types

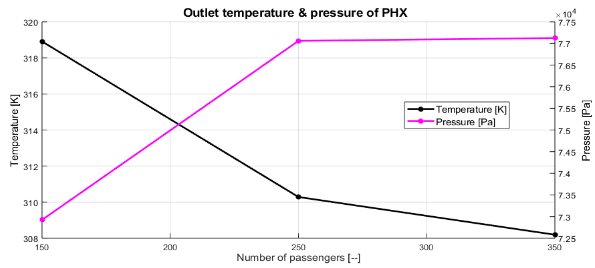

(a) Outlet temperature and pressure of the air - PHX

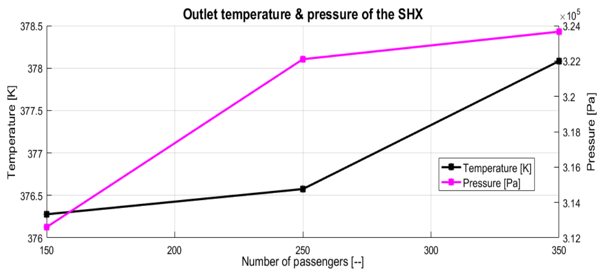

(b) Outlet temperature and pressure of the ram air- SHX

Fig. 11 . Heat Exchangers

Aircraft Type (–)	**L_{aS} (m)**	**L_{bS} (m)**	**L_{cS} (m)**
1	0.13	0.11	0.11
2	0.22	0.20	0.20
3	0.27	0.25	0.25

Table 13. Electric ECS - SHX geometry for three aircraft types

Compressed air passes through the ozone separator and flows into the primary heat exchanger (PHX). The primary heat exchanger is a cross flow type heat exchanger. The compressed hot ram air from ram air compressors is passed into the one side of the PHX and cold ram air from plenum passes on the other side of the PHX.
Table 12 & 13, represents the geometry of the PHX and SHX considered in this study for three aircraft types. The Figure 11a & 11b, represent the outlet temperature and pressure of air at the outlet of the PHX and SHX.

4.2.3 *Air Cycle Machine - Compressor*

The dimensional and thermal results are illustrated in Table 14 & Figure 12. These results are obtained analytically by solving the equations considered in the Section 3.1, Turbine sizing. The air inlet pressure of the Turbine is equal to the outlet air pressure from the SHX. The is-entropic efficiency of the compressor (η_{trb}) is considered to be 0.8. The slip factor of the compressor (S_{ftrb}) is 0.9.
From PHX the air flows into the ACM. In compressor, air gains the pressure and temperature. Table 14, Figure 12 are obtained using equation's considered in the Section 3.1. The pressure ratio of the compressor (π_c) is assumed to be 5. The specific heat of bleed air at constant pressure and volume is considered to be c_p=1.005 $(kj/kg.K)$ and c_v=0.716 $(kj/kg.K)$ [3]. The compressor efficiency (η_{cmp}) is assumed to be 0.7. The slip factor of the compressor (S_{fcmp}) is assumed to be 0.9. The impeller rotations per minute (rpm) (N_{cmp}) is considered to be 45000 rpm. The impeller inlet diameter (D_{1cmp}) is assumed to be half of the (D_{2cmp}).

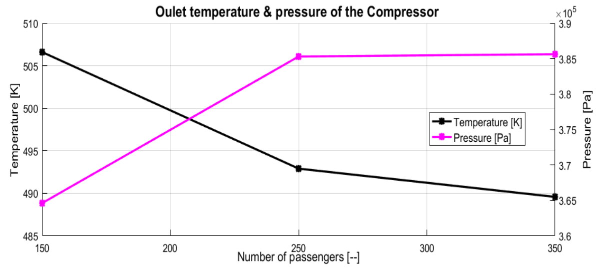

Fig. 12 . Outlet temperature and pressure of air at the exit of the compressor

Aircraft Type (–)	**outlet impeller Diameter D_2 (m)**	**inlet impeller Diameter D_1 (m)**
1	0.16	0.08
2	0.20	0.10
3	0.24	0.12

Table 14. The inlet and outlet geometry of the impeller in the compressor for the three aircraft types

4.2.4 *Air cycle machine - Turbine*

The dimensional and thermal results are illustrated in Table 15. These obtained by analytically solving the equations considered in the Section 3.1, Turbine sizing. The air inlet pressure of the Turbine is equal to the outlet air pressure from the SHX. The is-entropic efficiency of the Turbine (η_{trb}) is considered to be 0.8. The slip factor of the Turbine (S_{ftrb}) is 0.9.

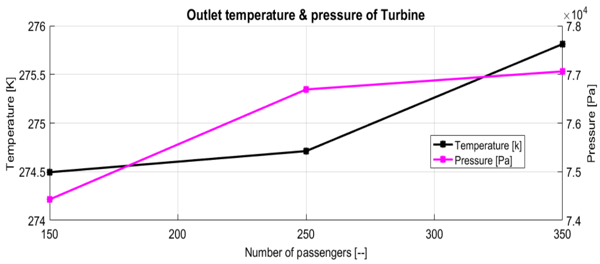

Fig. 13 . The temperature and pressure of the air at the exit of the Turbine

Aircraft Type (–)	**Outlet impeller Diameter D_2 (m)**	**Inlet impeller Diameter D_1 (m)**
1	0.12	0.06
2	0.16	0.08
3	0.19	0.095

Table 15. The inlet and outlet geometry of the impeller in the Turbine for the three aircraft types

4.3 Pressure Losses in Pipes

The hydraulic diameter (D_h) of each pipe differs for each type of aircraft, (D_h) for aircraft's type 1, type 2 and type 3 are 30 mm, 35 mm and 40 mm. The pipe is assumed to be made up of aluminum (Al). The absolute roughness of the pipe is considered to be $0.001*10^{-3}$ m [10]. Aluminum pipes are assumed for the calculations as they are cheap, the surface roughness ranges from $0.001*10^{-3}$ m to $0.002*10^{-3}$ m and are lesser in weight compared to the pipes made up of other metals.

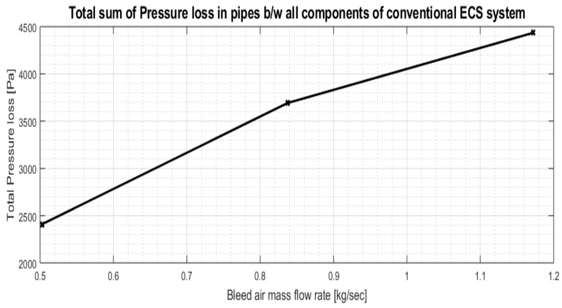

(a) Conventional ECS

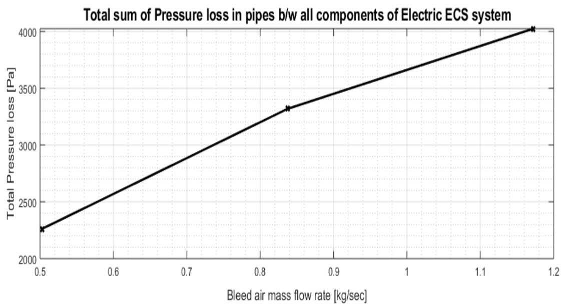

(b) Electric ECS

Fig. 14 . Sum of pipe pressure losses in all components

These characteristics of aluminum contribute economically and increase the efficiency of the system [10]. The pipe length between each component is considered to be 0.3 m. It is constant for both conventional and electrical ECS and does not vary with the type of aircraft.

The bend angle considered for each pipe connection for both conventional and electrical ECS is 90^0 and the bend type is flanged smooth bend. For the bend with an angle of 90^0 the flow is across bends, so the frictional factor value (K_L) is considered to be 0.3 [10]. Figure 14a & 14b, illustrate the sum of the pipe pressure losses for all the components of both conventional and electrical ECS.

4.4 Final pressure and temperature at the outlet of the conventional and electric ECS system

In this section, the plots represent the final temperature and pressure of the conditioned bleed air at the exit of the conventional and electrical ECS. Figure 15a & Figure 15b, represent the final pressure and temperature of the conventional ECS before the conditioned bleed air flows into the mixing manifold. Figure 16a & Figure 16b, represent the final pressure and final temperature of the electrical ECS at the exit of ECS and at the inlet of mixing manifold.

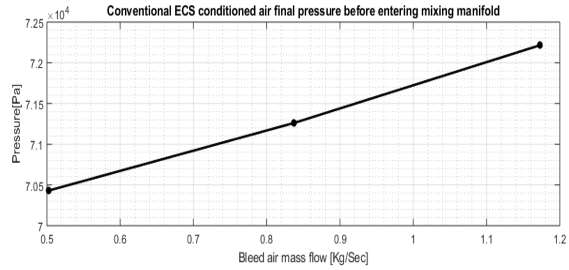

(a) Final pressure of the conditioned air at outlet

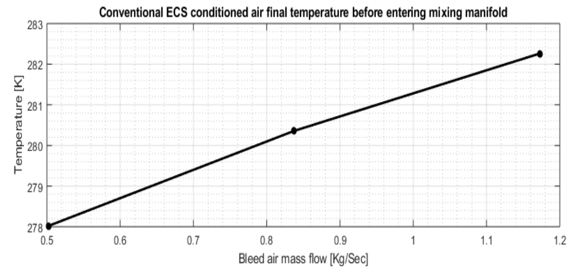

(b) Final temperature of the conditioned air at outlet

Fig. 15 . Conventional ECS

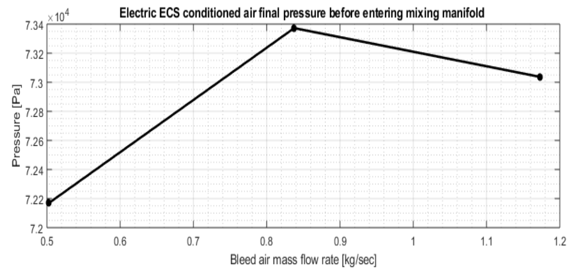

(a) Final pressure of the conditioned air at outlet

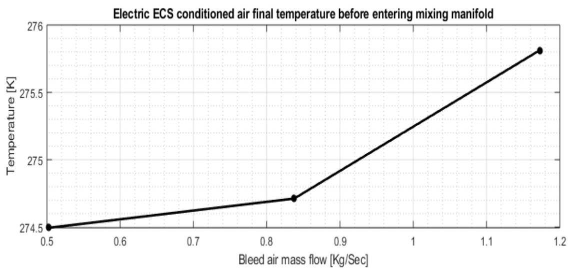

(b) Final temperature of the conditioned air at outlet

Fig. 16 . Electrical ECS

4.5 geometric models and RAPID Integration

Knowledge-based Engineering approach is employed in CATIA [11], the knowledge is stored in the form of templates also known as User Defined Features (UDF), these UDF's are instantiated repeatedly with the help of a catalog and Knowlege pattern to obtain the desired result. The geometric models of the two pack conventional and electrical ECS are represented in Figure 17a and 17b, respectively. These are the geometric models of ECS, that would be instantiated into the aircraft in RAPID [12] [13] and the choice of the system is controlled manually using a parameter. Essentially, the user can choose which system would be required for the particular aircraft.

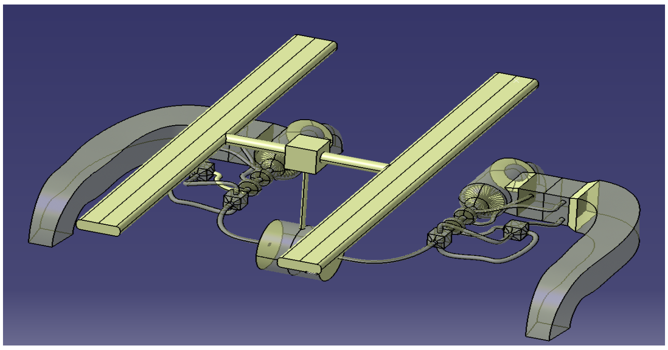

(a) Conventional ECS System

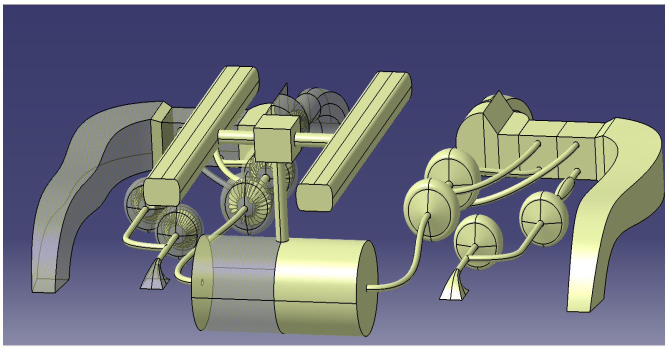

(b) Electric ECS System

Fig. 17 . Final ECS geometric models

The diffusers are connected to the main system through a mixing manifold. This air is then fed into the aircraft through the diffusers. The user has a controlling parameter to chose the type of ECS from and the sizing is done automatically based on the number of passengers that serves as the driving input.

The geometric model of the air diffusers is shown in Figures 18a that is integrated into the RAPID [12] [13]. Single-aisle configuration has the ducts that would be instantiated as shown. The number of diffusers to be instantiated into the aircraft can be controlled manually by a string parameter named "numberOfInstances" by the user as per the requirements. This parameter is controlled by the knowledge pattern code.

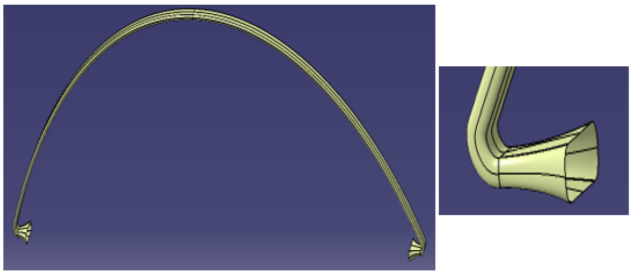

(a) Single aisle type diffuser ducts

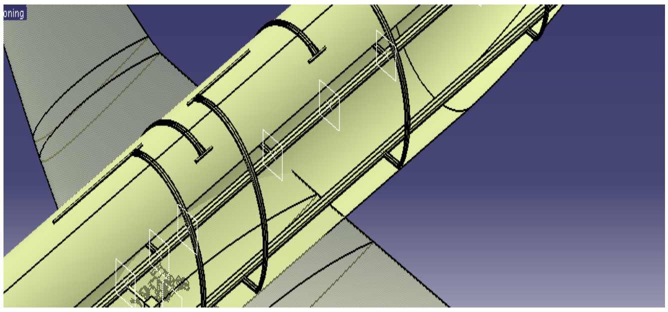

(b) Double aisle type air supply pipes

Fig. 18 . Single and double aisle diffusers configurations

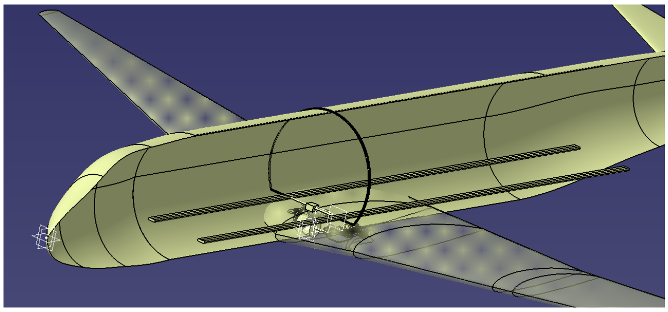

(a) Single aisle

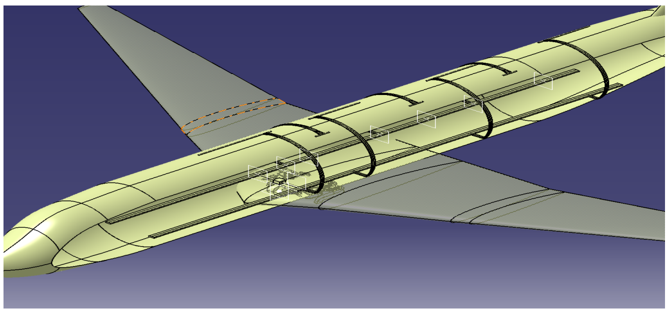

(b) Double aisle

Fig. 19 . Air supply piping in RAPID

Double aisle configuration is different compared to single-aisle, instead of diffusers, the system incorporates a different design. The air supply pipes are designed to ensure the supply of air to the cabin directly. Figure 18b shows the air diffuser pipes, that would also act as the ducts for the double aisle configuration. This eliminates the need for the ducts, in turn reducing the piping cost and the gross weight of tubing.

The different air supply piping are represented in Figure 19a & Figure 19b instantiated into RAPID [12] [13]. The user gets a parameter, which can be used to switch between the configurations for the aircraft. Figure 20, illustrate the ECS instantiated automatically into the RAPID. This automation is achieved by knowledge pattern scripting. The product knowledge template workbench is used for the implementation of knowledge pattern script into the CATIA model.

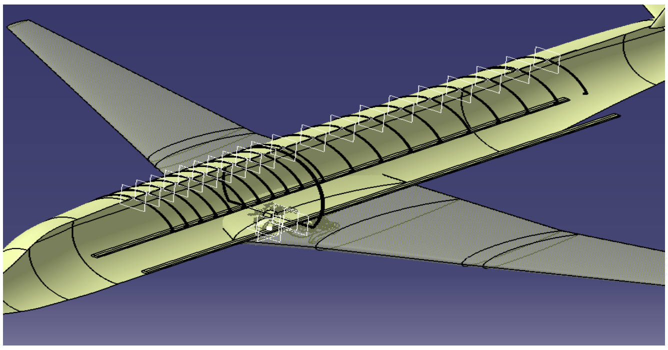

Fig. 20 . RAPID aircraft with ECS & single aisle ducts

5 Discussion

The automatic sizing of the ECS depends mainly on the number of passengers. This serves as the driving input and can be controlled using the equations in Section 3.1. This model is then integrated into the RAPID and can be tailored to meet the user requirements [12] [13].

From the results, it is observed that the conventional system results in a greater loss. This is due to the presence of bleed air in the system. Electrical ECS, on the other hand, utilizes electrical energy, thereby making it cleaner, energy efficient and greener. Thus, electrical ECS is the go-to choice these days and is used in Boeing 787.

The mass flow rate of bleed air depends on the number of passengers on the aircraft. Non-availability of data led to assumption of mass flow rate of 0.8 $((\frac{kg}{sec}))$ for 150 passengers. This value was increased by 0.3 $((\frac{kg}{sec}))$ for other aircraft types being considered. Initial sizing of the heat exchanger was done ensuring that the pressure loss would be in the range of 38,000 to 40,000 Pa. The sizing was done in iterations until the desired pressure loss value was obtained.

The number of tube passes (N_t), defined as the number of passes in a heat exchanger. This is usually measured across bleed and ram air flow directions and is obtained by [Equation 11]. The number of tube passes varies with aircraft type. Here it increases as aircraft type changes from 1 to 3. Parameters such as length of the heat exchanger(L_a), hydraulic diameter of fin tube (D_h) and longitudinal pitch (S_L) are used in formulating the number of tube passes (N_t).

Values obtained are cross-checked and verified with Liebherr data[8] for accuracy. From Figure 9, the variations can be observed between the Liebherr ECS data and Conventional ECS system data obtained in this study. In this study, we consider the bleed air to be ideal gas, the connecting pipe bend angle between the ECS components is assumed to be 90^0. The above mentioned assumptions in this study stand as a main reason for the variation between the Liebherr ECS data and Conventional ECS data obtained in this study. This serves as a validation for the assumptions made and final values of the design. Variations in the range 0.2 to 2.5 % are observed, these are within the permissible range. These results give the much-needed validation and provide the assurance that the design could be used for advanced models.

Aluminum is the preferred choice of pipe material for internal connection of ECS. The diameter of the pipe acts as a variable and varies with aircraft type. Pressure loss increases with an increase in the number of passengers in the aircraft. This might be due to the increase in mass flow rate of bleed air or due to constant pipe bend angle.

The geometric model of ECS and cabin air distribution system for single and double aisle cabin configuration are presented in Section 4.5. These models are parametric and knowledge pattern was used in automation. The user has the complete freedom to alter the final design by controlling or changing a few parameters. Knowledge pattern scripting controls the design in RAPID, based on user inputs. The scripting is faster and flexible when compared with VBA [14]. The number of air ducts for the single-aisle configuration can be adjusted or controlled by a few parameters. The design being really flexible can be customized easily for either single or double aisle configuration.

6 Conclusion

Analysis and working of conventional and electrical ECS are addressed along with temperature and pressure data for different aircraft configurations. These systems are designed and tested for different aircraft types with a different number of passengers. The temperature and pressure data obtained from the system for a specific cruise altitude are compared with the standard data for accuracy. Results show a minor variation from the standard values, although this could be accounted for the constants that are assumed during the course of the calculation. This work can be taken as the first step in ECS and can serve as the base for further improvements, including increasing the size for an extremely high or low number of passengers.

REFERENCES

[1] Moir I and Seabridge A. *Aircraft Systems: Mechanical, electrical and avionics subsystems integration*. Aerospace Series, 3rd ed. John Wiley and Sons, Chichester, 2008.

[2] Peng X. *Aircraft Environmental control systems modelling for configuration selection*. MSc thesis, Cranfield University, 2013.

[3] Incropera F P and DeWitt D P. *Fundamentals of heat and mass transfer.* New York : Wiley, cop. 2002 (dvs 2001), 2002.

[4] Amrutkar P S, Patil S R and Shilwant S. *Automotive Radiator-Design and Experimental Validation*, vol. 3. 2013.

[5] Feliot P, Guennec Y L, Bect J and Vazquez E. *Design of a commercial aircraft environment control system using Bayesian optimization techniques*. 2016.

[6] Kangsoo I M. *Development of a design method for Centrifugal Compressor*. Michigan State University, 2012.

[7] Perez Linares D. *Modeling and simulation of an aircraft environmental control system*. 2016.

[8] Liebherr. *Airbus A319/AIRBUS 320/A321 ECS Training Manual*. 2004.

[9] Vega Diaz R. *Analysis of an electric environmental control system to reduce the energy consumption of fixed-wing and rotary-wing aircraft*. Cranfield University, 2011.

[10] Miller D S. *Internal flow systems.* Cranfield : BHRA (Information Services), cop. 1990, 1990.

[11] Catia®V5. 3d cad design software, dassault systémes, 2016. [Online; accessed: 2016-09-06]. URL `http://www.3ds.com/products-services/catia/`

[12] Munjulury R C, Staack I, Berry P and Krus P. A knowledge-based integrated aircraft conceptual design framework. *CEAS Aeronautical Journal*, vol. 7, no. 1, pp. 95–105, 2016.

[13] Munjulury R C. *Knowledge-based integrated aircraft design: An applied approach from design to concept demonstration*, vol. 1853. Linköping University Electronic Press, 2017.

[14] Aakash S, Govindarajan V K, Munjulury R C and Krus P. Knowledge based design methodology for generic aircraft windshield and fairing-a conceptual approach. *51st AIAA Aerospace Sciences Meeting including the New Horizons Forum and Aerospace Exposition*. American Institute of Aeronautics and Astronautics, Grapevine, Texas, USA, 2013.